FINAL REPORT

STUDY OF A TRUSSED GIRDER COMPOSED OF A REINFORCED PLASTIC

by

Fred C. McCormick
Faculty Research Engineer
Virginia Highway & Transportation Research Council

and

Professor of Civil Engineering
University of Virginia

SUMMARY

The structural behavior of a series of laboratory test specimens was investigated to determine the ultimate strength, the deformation characteristics, and the mode of failure of a trussed girder composed of glass fiber reinforced polyester resin. Computations based on classical theories of elasticity were made for comparison with experimental results. Reasonably good agreement was noted between the theoretical calculations and the experimental observations. Efforts to eliminate adhesive failures at the joints appeared to be successful in the last specimen fabricated and tested. A maximum live-load to dead-load ratio of 93 to 1 was achieved in the series of load tests.

A study of the weathering characteristics of reinforced plastics indicated that rapid degradation of mechanical properties may occur under normal outdoor exposure conditions. There are no completely reliable means available at this time to accurately predict the service life of a given structure composed of reinforced plastics, but considerable effort and progress are continuing in several sectors to improve both materials and performance predictability.

608

FINAL REPORT

STUDY OF A TRUSSED GIRDER COMPOSED OF A REINFORCED PLASTIC

by

Fred C. McCormick
Faculty Research Engineer
Virginia Highway & Transportation Research Council

and

Professor of Civil Engineering
University of Virginia

INTRODUCTION

The applications of reinforced plastics as primary load-bearing structural members have increased in recent years in the building construction industries.[1,2,3,4] Many applications have been made to meet the specialized requirements of a particular service, but all have provided either direct or indirect cost benefits to the user.[5] Among the attractive features of the materials systems thus utilized have been high strengths, low weights and industrialized fabrication capabilities. In light of the paucity of similar applications in the highway industry, and in particular highway structures, a study was made of ways to adapt high performance plastic composites to beneficial uses in highway structures.[6] After consideration of the various aspects of the materials utilization question, a research program was initiated to develop a flexural member which would be suitable for a primary load-bearing component in a bridge structure. This report, therefore, deals with the design, fabrication and load testing of a selected flexural member composed entirely of glass-reinforced plastic. A study of the literature related to weathering of polymeric materials was also made and is included herein.

Some of the findings from a previous investigation are included for comparative purposes and discussion in this report (see "Initial Studies of a Flexural Member Composed of Glass-Fiber Reinforced Polyester Resin", VHRC Report 73-R3, July 1973).

RESEARCH OBJECTIVES

The objectives of the research reported here were to:

1. Design a flexural member which would take advantage of the high strength characteristics of glass fibers.

2. Maximize the live-load to dead-load ratio.

3. Fabricate a test specimen with a size and geometry representative of some in-service structural members.

4. Obtain data relative to the stiffness, strength and stability of the specimen by load testing.

5. Evaluate load performance characteristics and manufacturing feasibility of the flexural member.

6. Assess weathering characteristics of reinforced plastic composites.

These objectives were achieved to varying degrees during the period of investigation from September 1973 to June 1974.

DESIGN OF THE FLEXURAL MEMBER

The approach to the design of the flexural member was dictated by the highly orthotropic characteristics of the composite material used. (7,8,9) In order to exploit the high tensile strength property of the glass fibers, it was desirable to utilize an arrangement wherein the fibers would be axially aligned with the direction of the tensile stresses in the member. This criterion could be satisfied in the lower chord and diagonal web elements of a Pratt truss configuration, so initial consideration was given to truss geometries. It was also recognized that the highest material efficiencies could be achieved by a filament-winding process (i.e., the process of building up a cross-sectional area by repetitive passes of continuous strands of resin-impregnated glass fibers) in which material volumes would be closely matched with strength requirements from point to point throughout the member. However, a filament-wound composite is usually inefficient in resisting compressive (buckling) stresses so the winding process was not suitable for the top chord. (10)

Geometric Considerations

With the above limitations and advantages in mind, an initial shape was adopted which would combine the features of both an open-web truss and a solid-flange girder. This combination would include built-up elements of filament-wound fiber glass for the web diagonals and lower chord and solid, prefabricated plate and rod shapes for the top chord and vertical web elements. Lateral and torsional stability for the member was provided with a biplanar arrangement of the web elements and a common lower chord, i.e., a triangular cross section. A sketch of the initial concept is shown in Figure 1. The combination of the geometry and behavioral concepts gave rise to the designation of Triangular-Trussed-Girder (TTG) for the integrated structural member.

An eight-foot (2.4m) long member was selected for a laboratory test specimen based on available material dimensions and the capacity of the loading fixture. Other geometric dimensions were established in accordance with the following guidelines and principals.

1. The length to depth ratio usually ranges from 6 to 8 for highway bridge trusses.

2. Lateral deflections would be resisted by the top plate and the component of the inclined truss projected into a horizontal plane.

3. Resistance to in-plane distortion is inherently high in an equal-angle triangular cross section.

4. The spacing of the vertical web elements required a balance between the unsupported length of the top plate and the amount of material required for the diagonal web and lower chord elements.

Stress Considerations

The first three test specimens were designed with the longitudinal spacing of the vertical web elements based on the shape of the bending moment diagram for a uniformly loaded beam such that the cross-sectional areas of the chord elements would increase by the same increment in each panel to satisfy the flexural stress requirements. For a uniformly loaded (w), simply supported member of length L, the moment increase in each panel is $1/32wL^2$ from the end toward the center. For lack of a better approach, the cross-sectional areas of the individual elements were determined from a simplistic stress analysis of the entire member acting as a pinned-end truss. The dimensions and details shown in Figure 2 resulted from this analysis coupled with intuitive judgment of the interaction of the elements of the member. As will be shown later, this assumed behavior was close to experimental observations. The initial specimen was designed for a total uniformly distributed load of 10,000 pounds and a load safety factor of 2. The required areas of the elements were determined as shown in Table 1 using material properties of ultimate tensile stress at 100 ksi (690 MPa) and comprehensive stress at 35 ksi (241 MPa). The areas actually provided were somewhat different due to fabrication considerations.

From the detailed sketches of the joints shown in Figure 2, it can be seen that no special efforts were made in the first speciment (TTG-1) to ensure the integrity of the connection at the top and side plates other than that provided by the resin used in winding. Consequently, it was expected that separation of the plates would occur at a low load. This, in fact, happend and various procedures were investigated subsequently to strengthen the joint. No effort was made to predict elastic deflections in the preliminary calculations because the behavior of the intersecting joints of the elements and the true value of the elastic moduli of elasticity were unknown.

As each specimen was loaded to failure, design modifications were made in subsequent specimens based on a finite element stress analysis of the member and the observed mode of failure. A brief description of the computer program used for the analysis is included in Appendix A. These modifications resulted in changes which are discussed in the following section.

¼" flat plate bonded to top flange plate

¼" top flange plate

3/8" square rods for ver-tical web elements.

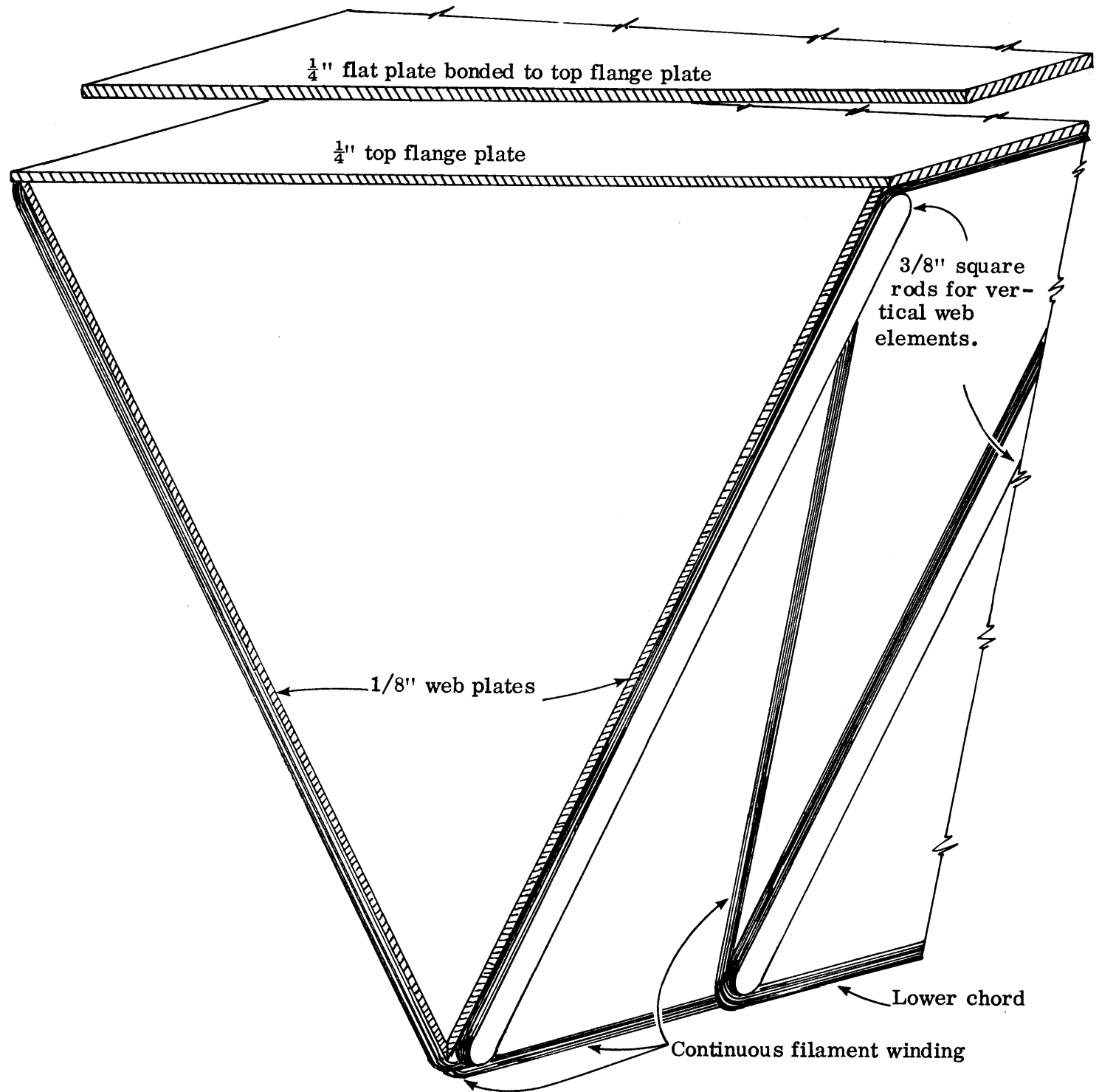1/8" web plates

Lower chord

Continuous filament winding

Figure 1. Sketch of TTG-1 flexural member showing filament winding, top flange plates and vertical web stiffeners. **Basic conversion unit: 1"=25.4mm.**
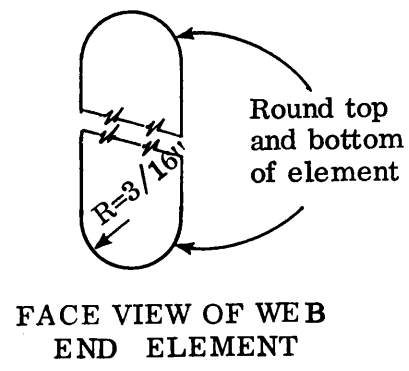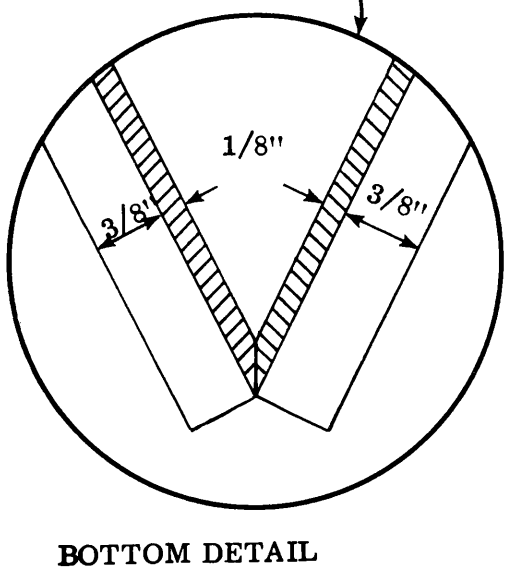
4'0" (one half length)

11 3/4"

3/8" square vertical web elements

½"   6½"   7¼"   103/8"

SIDE VIEW OF GIRDER

12"

11 3/4"

END VIEW

5/16"

TOP PLATE

¼"
¼"

1/8"   3/8"

Side Plate

Web element

TOP DETAIL

1/8"

3/8"   3/8"

BOTTOM DETAIL

Round top
and bottom
of element

R=3/16"

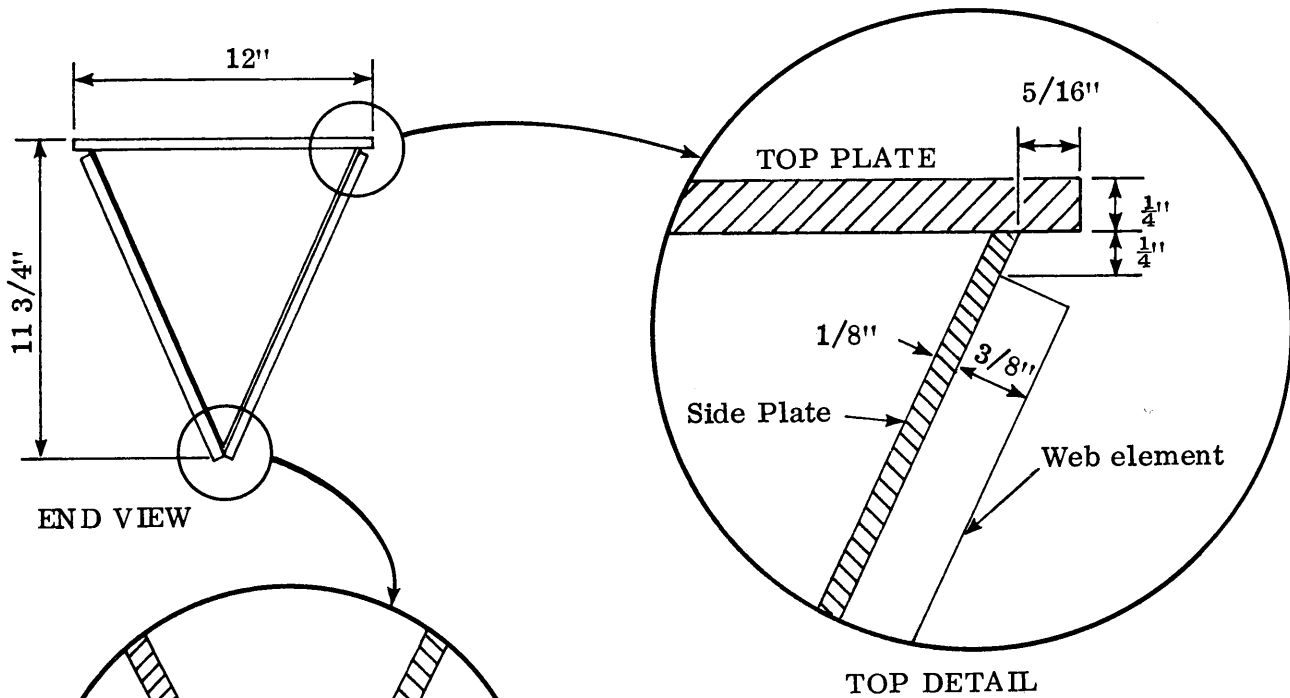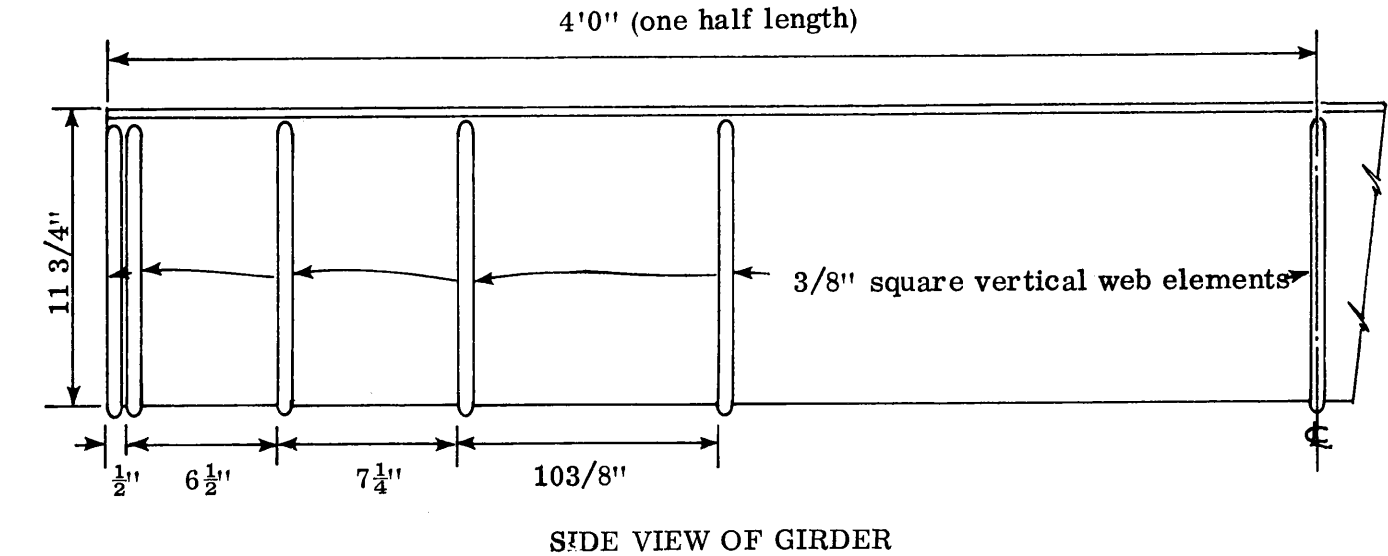FACE VIEW OF WEB
END ELEMENT

Figure 2.   Details of TTG-1 (skeletal frame prior to winding).

Basic conversion unit: 1"=25.4mm.

TABLE 1

COMPUTED AND SUPPLIED AREAS FOR ELEMENTS OF TTG-1

Basic conversion unit: $1 \text{ in}^2 = 645.16 \text{mm}^2$.

Element	Required Area (Square Inches)	Supplied Area (Square Inches)
Web, Each Side		
$U_1 L_1$	0.160	0.28
$U_1 L_2$	0.064	0.06
$U_2 L_2$	0.160	0.28
$U_2 L_3$	0.056	0.06
$U_3 L_3$	0.137	0.28
$U_3 L_4$	0.052	0.06
$U_4 L_4$	0.082	0.28
$U_4 L_5$	0.063	0.06
$U_5 L_5$	0.080	0.28
Top (flange plate)		
$U_1 U_2$	0.144	6.00
$U_2 U_3$	0.288	6.00
$U_3 U_4$	0.440	6.00
$U_4 U_5$	0.532	6.00
Bottom Chord		
$L_1 L_2$	0.050	0.04
$L_2 L_3$	0.100	0.15
$L_3 L_4$	0.150	0.24
$L_4 L_5$	0.200	0.36
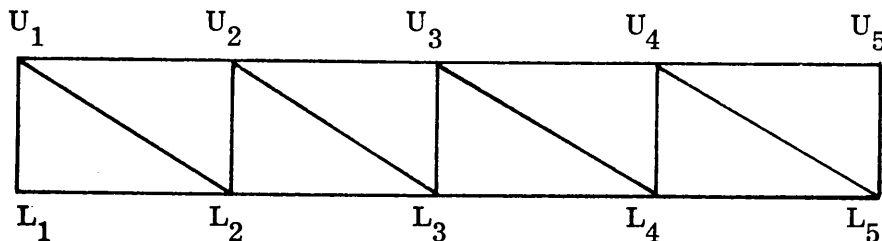
Legend for one-half of member

FABRICATION OF TEST SPECIMENS

Materials

The materials used in the test specimens included the following principal items:

1. Glass fiber reinforcing, 30-end equivalent roving of E glass;
    manufactured by Pittsburgh Plate Glass for the first three specimens.
    other specimens contained Owens Corning Fiberglas roving, Type 30,
    E glass.

2. Polyester resin 2036 (with MEK peroxide catalyst) with a gel time of
    about 45 minutes and room temperature cure; manufactured by
    North American Rockwell Company.

3. Prefabricated plates and shapes of EXTREN 500, manufactured by
    Morrison Molded Fiber Glass Company.

Fabrication Procedure

A total of seven test specimens were fabricated in laboratories at the University
of Virginia. TTG-1 was processed by joining the three plates with adhesive tape to form
the triangular shape and then attaching the 3/8-inch (1cm) square rods to the side plates
with spots of polyester resin at each end. After the resin was cured for at least twenty-
four hours, the lower chord and web members were formed by winding impregnated glass
roving around the ends of the stiffeners in a specified pattern which provided the desired
cross sectional areas. Five major winding patterns were followed to develop the areas listed
in Table 1. The top plate and vertical web members had constant cross-sectional areas be-
cause of the fixed minimal dimension of the prefabricated shapes. Larger prototype members
would permit the variation of these areas to conform better to the calculated stress requirements
for the member. No cross stiffeners were used to distribute the test load to the web members
at the panel joints.

Specimen 2 (TTG-2) was fabricated in the same manner as TTG-1 except that the
joints between the plates were strengthened by bonding one-half of a 6-inch (15 cm) wide strip of
chopped fiber mat to the face of each of the plates along the length of the joint. The size
of the outstanding dimension of the vertical web elements was increased to 3/4 inch (2 cm) to
provide more space for the roving. This increased the area of the vertical stiffener to a
value considerably in excess of that required.

Specimen 3 (TTG-3) was fabricated in a manner similar to TTG-2, but with two
modifications. First, the mat used to reinforce the plate joints in TTG-2 was replaced
with a prefabricated EXTREN angle (1 1/2" x 1 1/2" x 3/16") (3.8 x 3.8 x .5 cm) which was
bonded initially to the top plate and subsequently to the top ends of the vertical web elements.
Secondly, the web plates were removed from the member after winding to leave an open-web
structure which was bonded with polyester resin to the angles on the top plate. Some slight
changes were also made in the winding pattern to improve the technique and time requirements for
the process. Sequential photographs of the fabrication of the specimen are shown in Figures 3
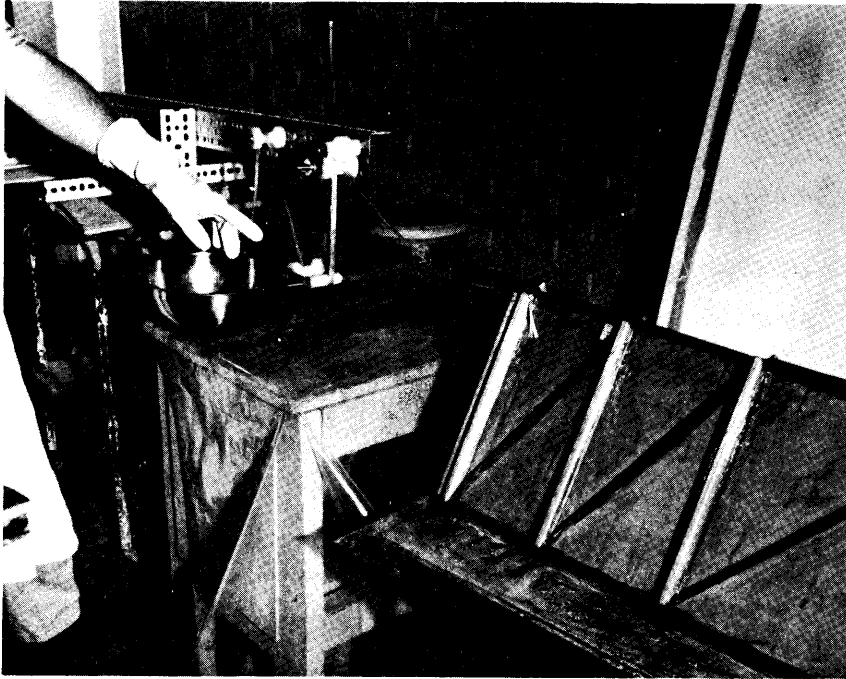through 6.

Figure 3. View of TTG-1 and the equipment used for impregnating the glass fibers with resin.
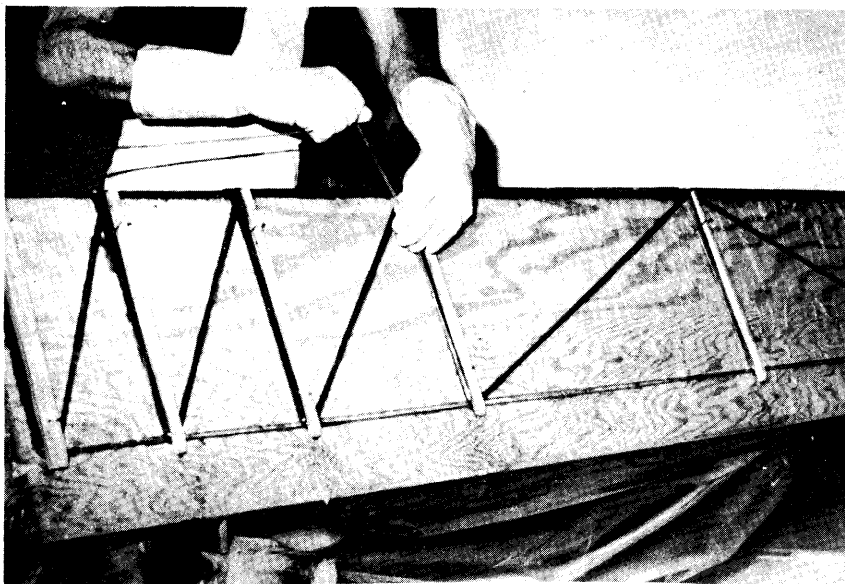

Figure 4. Winding the web and chord elements of TTG-3 on a **removable** wooden form.
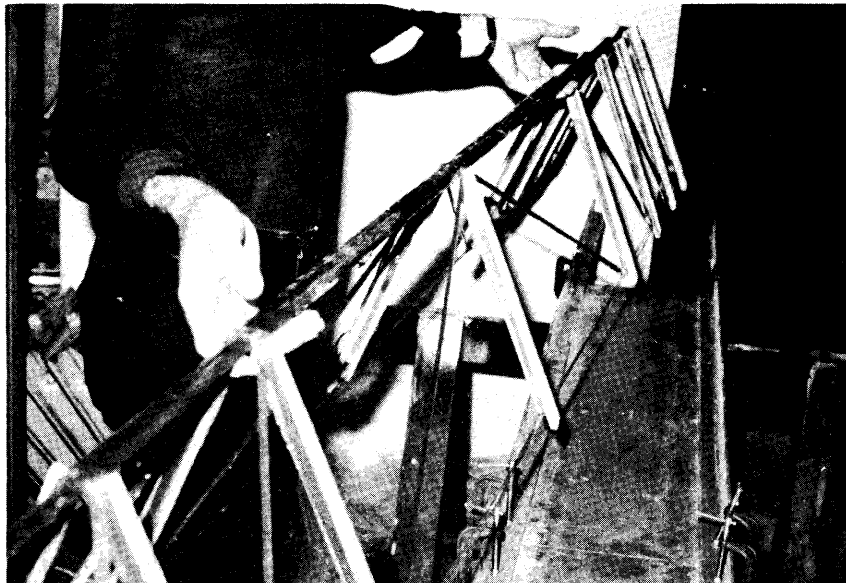
Figure 5. Completed web and chord elements of TTG-3 prior to attaching to the top plate assembly.

Figure 6. Application of resin binder for top cover plate on TTG-3.

Following a failure of TTG-3 (discussed in a following section) due to gross movement of the top end of a vertical web element, the specimen was strengthened by winding roving around the top ends of the vertical stiffeners in the plane of the top flange. It was anticipated that the additional roving would prevent movement of the stiffeners with an application of load. The modified specimen was designated as TTG-3M.

Specimens 5 through 7 (TTG-4, TTG-4R, TTG-5) were fabricated in a manner similar to TTG-3 with respect to the lower chord and web elements, except that all panel lengths were equal in length. The upper flange assembly was entirely different, however, and represented a major change in the design concept. Figure 7 shows the basic features of the top flange assembly for TTG-4. Specimen TTG-4R was identical with TTG-4 except for the elimination of the two 1/2-inch (1.3 cm) square rods which connected the channel elements. The flange plates were bonded directly to the channel elements in TTG-4R. Specimen TTG-5 represented another major change in design concept in which the transverse channels were connected mechanically to the top flange plate with five strands of glass roving prior to attaching the vertical stiffeners and winding the lower chord and web elements. This assembly is shown in Figure 8. Upon completion of the lower chord and web elements, five strands of roving were wound circumferentially around the member at each panel point. These strands resisted the lateral movement of the top ends of the stiffeners and permitted the elimination of the edge angles used in previous specimens.

It should be noted that the specimens were fabricated by personnel with no previous experience in fabrication techniques and with no specialized equipment for handling the materials. All bonding and winding procedures were performed manually by two individuals working together. Tension of the strands was not measured but efforts were made in specimens subsequent to TTG-2 to keep the strands as tight as possible by hand. As experience was gained, the techniques improved rapidly and the winding operation which required two days for the first specimen required only one and one-half hours for the last specimen.
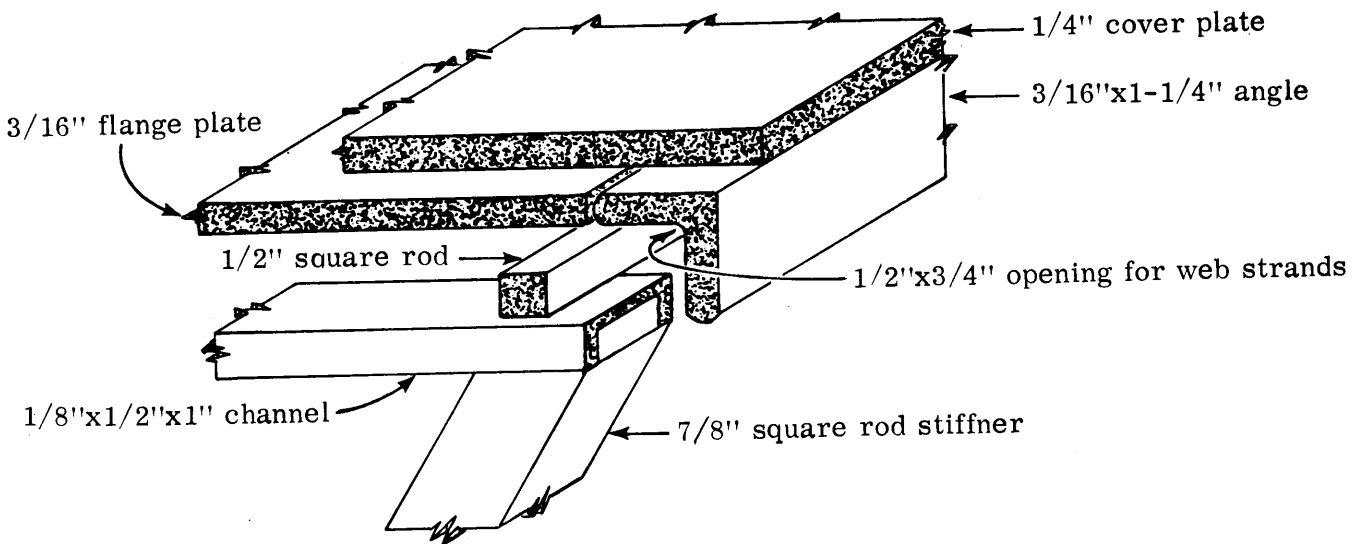

Figure 7. Top-flange assembly details of specimen TTG-4R. Basic conversion unit: 1"=25.4mm.
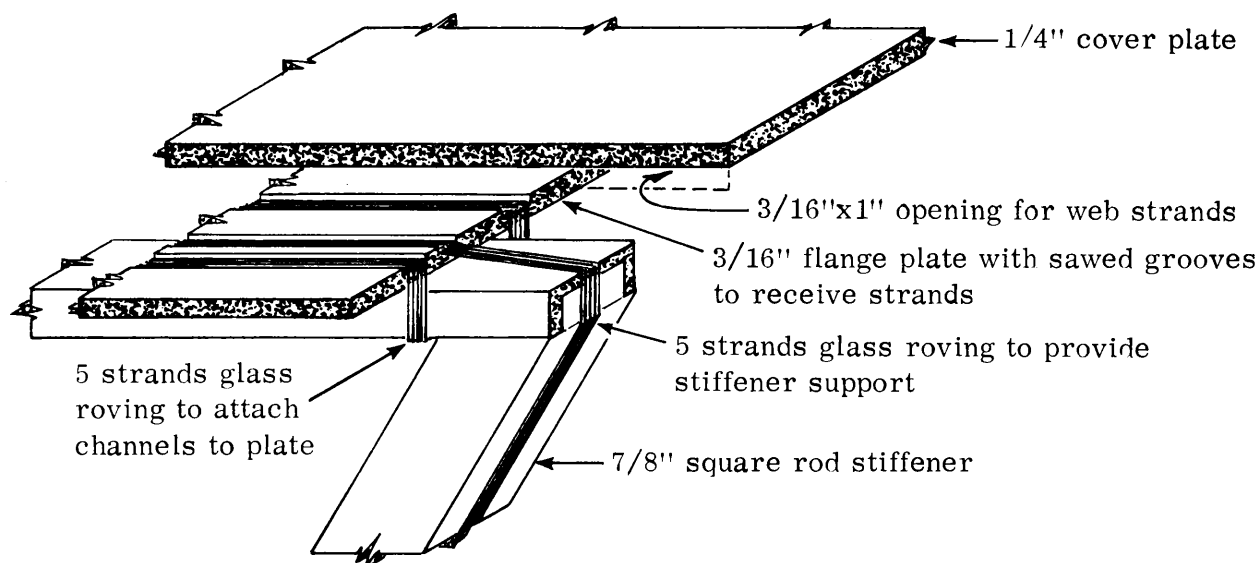
1/4" cover plate

3/16"x1" opening for web strands

3/16" flange plate with sawed grooves to receive strands

5 strands glass roving to provide stiffener support

5 strands glass roving to attach channels to plate

7/8" square rod stiffener

Figure 8. Top-flange assembly details of specimen TTG-5. Basic conversion unit: 1"=25.4mm.

TEST PROGRAM FOR THE STRUCTURAL MEMBERS

Instrumentation

Test specimens were instrumented to obtain data for vertical deflections and strains in selected elements during loading. All deflection measurements were made with conventional dial indicators with least readings of 0.0001 inch (0.025 mm). Strains were measured by means of electrical resistance strain gages bonded to the surface of the web and chord elements. Gages supplied by the Micro-Measurements Company, types EA-06-250 BF-350 and EA-06-250 TB-350, were bonded with MM A/E-10 epoxy adhesive to TTG-1 and with M-bond 200 adhesive to all other specimens. In addition, several three-element wire rosette gages were bonded to the side plates of specimens TTG-1 and TTG-2 to monitor the buckling behavior of the plates. Strains were recorded by means of a 50 channel, Model 205 indicator and Model 305 switching system made by William T. Bean, Inc.

Load Testing

All load testing was performed in the structural test laboratory of the Department of Civil Engineering at the University of Virginia. Test loads were applied with hydraulic cylinders connected to a Riehle/Los pumping console which provided load control to the nearest 80 pounds (356 N) per cylinder (10 psf (479 N/M²)uniformly distributed load on the member). An air bag 3 x 9 x 1-foot deep, (0.92 x 2.75 x 0.3m) made by the Uniroyal Company, was used to spread the load uniformly over the top plate of the member. Different views of the load test arrangement are presented in Figures 9 and 10. Support was provided at the ends of the test member by wooden frames built to fit the triangular shape of the cross section. A 1/4 inch (0.63 cm) thick strip of elastomeric material was attached to the support frame to ensure distributed contact along the sides of the "V" of the support frame
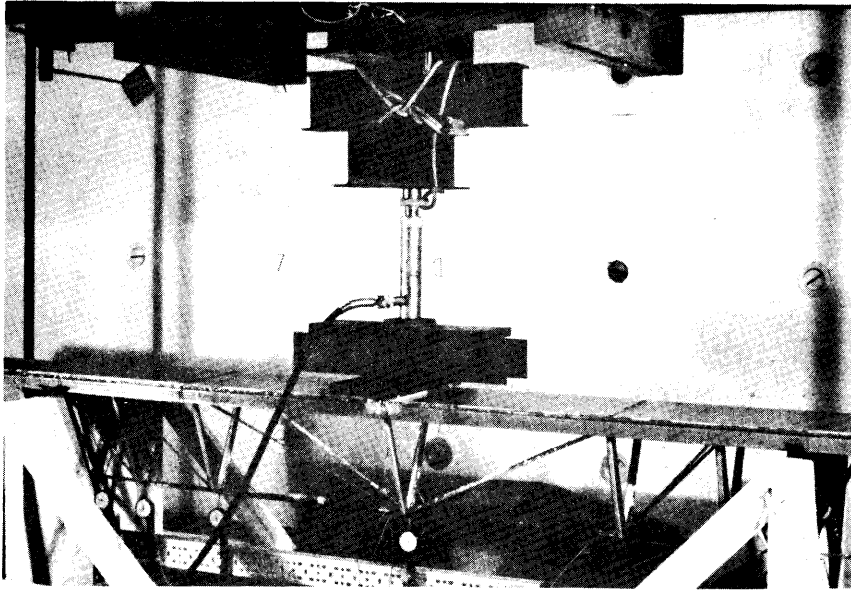
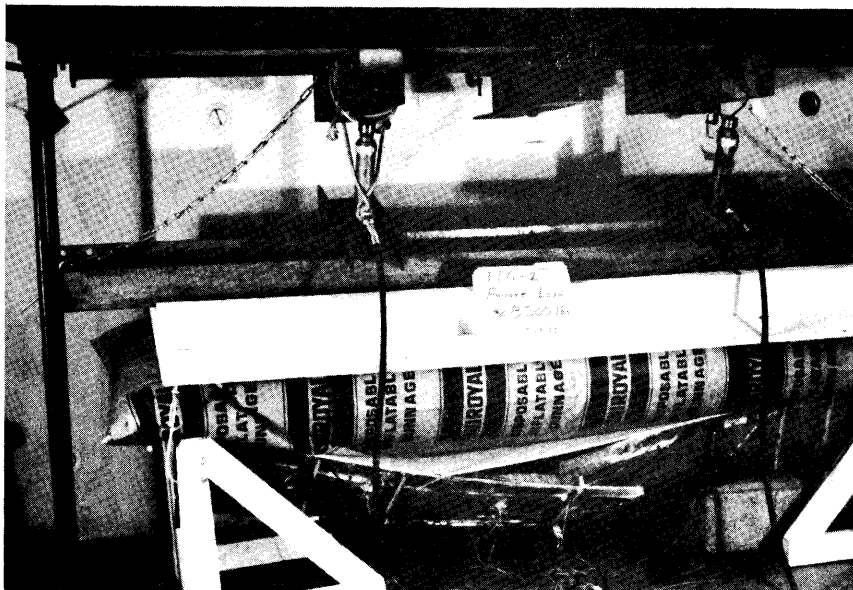**Figure 9.** Typical reduced span arrangement with center point load applications.

Figure 10. View of TTG-2 at the ultimate load.

and the vertical web elements at the ends of the member. In order to prevent in-plane distortion of the end sections at high loads, 3/4-inch (2 cm) thick wooden diaphragms were fitted inside the test specimen at the points of support. Several reduced span load tests were also conducted by locating the support frames and diaphragms at intermediate panel points. Both distributed and single-point loads were used for these tests. No measurements were made to determine the amount of rotation which occurred at the supports during load applications, i.e., to ascertain the degree of restraint at the support, but visual observations of the member indicated that no obvious end restraint was present. No effort was made to control the environmental conditions during the period of load testing. In general, the temperature ranged from 68 to 75° F (20-24° C) and the relative humidity from 45 to 65 percent.

EXPERIMENTAL TEST RESULTS AND DISCUSSIONS

Mechanical Properties of the Composite Material

The mechanical properties used for designing the first test specimen were taken from average values recommended by the plastics industry. However, in order to compute theoretical stresses and deflections for comparison with the load test results, it was necessary to determine the elastic tensile modulus of the as-fabricated composite material. Consequently, upon the completion of testing several of the specimens, a portion of the lower chord element was removed and loaded in uniaxial tension in a Baldwin-Lima-Hamilton hydraulic universal testing machine to obtain the stress-strain data shown in Figure 11. The strain data were obtained independently with a bonded electrical resistance gage and a mechanical extensometer at various load increments.

The first modulus data obtained from TTG-2 appeared to be bilinear with a change in slope at a stress of 10,000 psi (69 MPa). The tensile modulus of 4.6×10^6 psi (31 GPa) above the 10,000 psi (69 MPa) stress was within the industry range of 2.3 to 6×10^6 psi (16 to 41 GPa) but appeared low for a composite with fully oriented glass fibers. A composition analysis of this specimen by an ignition test indicated a glass content of 51 weight percent glass. This was quite low when compared with an industry-wide range of 75 to 85 weight percent glass for similar materials. Efforts therefore were made to decrease the resin content by passing the impregnated roving through a resin stripping die as it emerged from the resin bath. Additional attention was also given to maintaining a constant and uniform tension in the strands as they were wound into position in the web and lower chord elements. These changes in the fabrication procedures (as indicated in Figure 11) improved the moduli and glass contents. However, the glass contents remain below industry achievement and may represent an upper limit in the manual fabrication procedure.
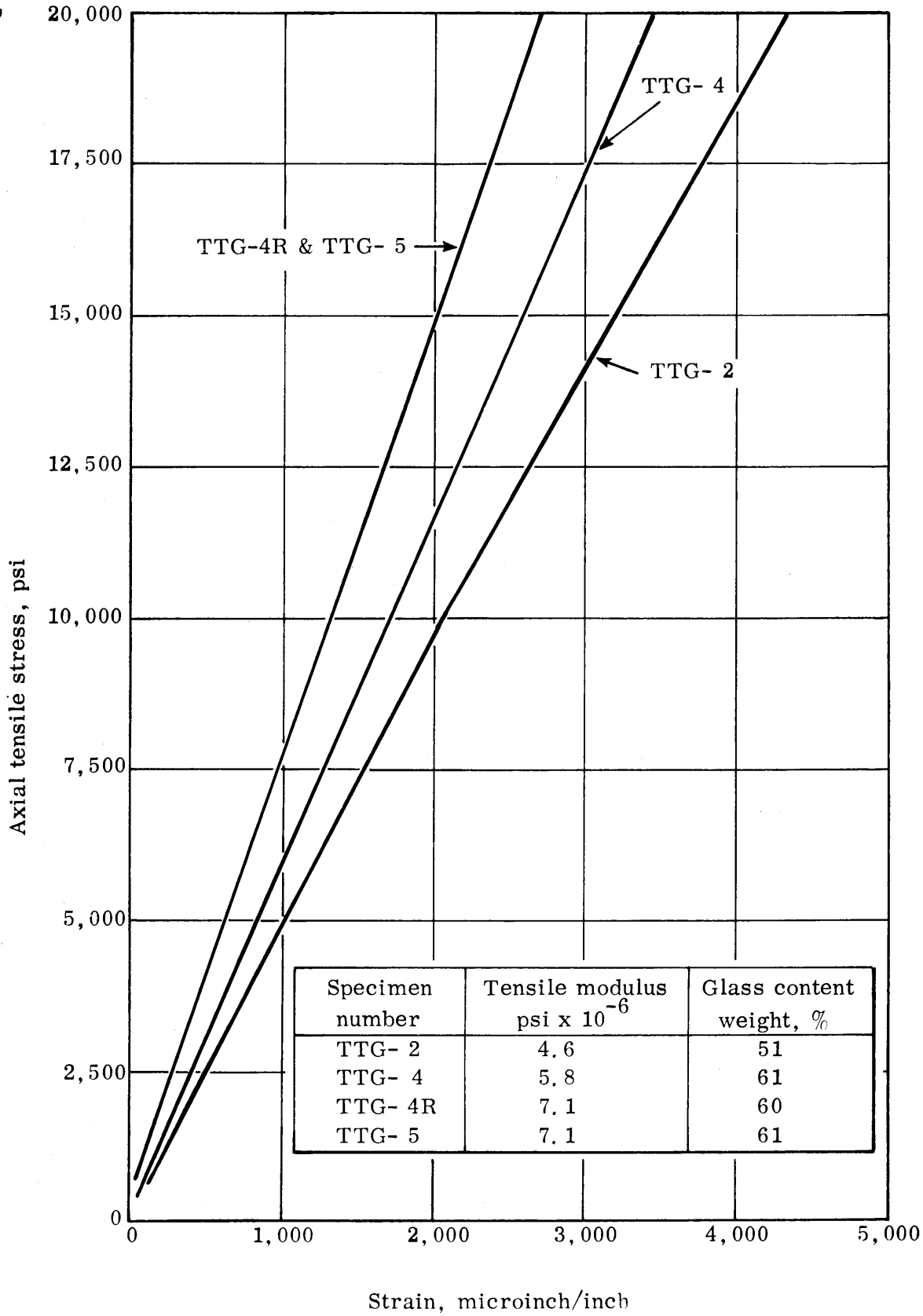
Figure **11.** Uniaxial stress-strain relationship and composition of bottom chord elements.

Axial tensile stress, psi

Strain, microinch/inch

TTG-4

TTG-4R & TTG-5

TTG-2

Specimen number	Tensile modulus psi x 10^{-6}	Glass content weight, %
TTG- 2	4. 6	51
TTG- 4	5. 8	61
TTG- 4R	7. 1	60
TTG- 5	7. 1	61

Strength Characteristics and Failure Modes

The ultimate strength of the primary elements (top plate, web and lower chord) was not fully tested in any of the specimens because of the failure of various joints. Failures of the test specimens were characterized by sudden changes in load carrying capabilites due to either rupture or excessive movement of an element resulting from an adhesive bond failure. Table 2 lists the failure load and mode for each of the seven specimens.

Initial failure in TTG-1 occurred at relatively low vertical loads (1,260lb.) (5.6KN) in the end panels when the adhesive bond at the joint ruptured and permitted a lateral translation of the web plates. Upon removal of the test load, the member regained its shape with no apparent damage to other elements. Therefore, the joint was repaired by winding five strands of resin impregnated roving circumferentially around the entire member at panel points L_2, L_3, and L_4. A second load test reached approximately 3,260 lb. (14.5KN) before the joint in the center panel debonded and the web plates moved outward on both sides.

As mentioned previously, the joint between the web plate and the top plate of TTG-2 was reinforced with a strip of chopped glass mat bonded across the joint. Failure of this member was sudden at a load of 9,160 lb. (40.7 KN). It appeared to initiate with a bond rupture along the mat-web-plate interface and the center joint in the web plates opened and ripped the mat as shown in Figure 10. The two top plates were also separated with bond failure at the interface.

Specimen TTG-3 failed at 2,660 lb. (11.8KN) due to movement of one of the vertical web elements in a longitudinal direction. The resin provided insufficient restraint at the top of the web element in the adjacent panel. After providing additional reinforcement to the top plane of TTG-3 (as described previously and redesignated as TTG-3M), a total load of 4,000 lb. (17.8 KN) was applied before failure occurred at the upper end of a stiffener at panel U_2. This element split due to the axial force exerted by the strands of web element U_2L_3 in contact with the unprotected end of the stiffener. Failure to protect the end of the rod from the splitting action of the strands was an oversight and easily corrected by the modifications subsequently made in specimen TTG-4.

Failures of both specimens TTG-4 and TTG-4R were initially attributed to plane shear at the interface between the flange plate and the rod or channel shapes attached to the stiffeners. However, this type of failure could not be justified logically on the basis of the anticipated strength of the adhesive of several thousand psi and the computed shear stress of 131 psi (900 KPa) at the point of failure. It was concluded that the joint was undergoing considerable multidirectional distortion during loading and that the adhesive bond was failing due to very high tensile stresses located at the tip of a crack propagated by a prying action of the mating parts. Redesign of specimen TTG-5 to resist separation of the channel and plate in directions normal to their surfaces appeared to verify this conclusion and to correct the bond failure problem in the joint. Thus, the ultimate load of TTG-5 was increased by fifty percent over TTG-4R and the failure point was shifted to the light-gauged channel section which was subjected to the thrust of the vertical stiffener at U_2.

TABLE 2

Ultimate Loads and Failure Modes of Test Specimens

Basic conversion units: 1 psf = 0.48 KN/m^2

1 pound = 4.45 N

Specimen Number (1)	Ultimate Load on Member, in Pounds per Square Foot (2)	Failure Mode (3)
TTG-1	408	Web plate displaced laterially at top when bond failed between top and web plates.
TTG-2	1,146	Adhesive bond failure along the top mat-web plate interface.
TTG-3	333	Displacement of vertical stiffener due to bond failure at top of stiffener.
TTG-3M	533	Splitting of vertical stiffener U_2L_3.
TTG-4	326	Bond failure at the interface between the top plate and stringer.
TTG-4R	407 *	Bond failure at the interface between the top plate and the transverse channels.
TTG-5	575 *	Rupture of a transverse channel due to large force from the vertical stiffener.

* Weights of TTG-4R and TTG-5 were 57.6 and 49.6 pounds, respectively.

Stiffness Characteristics

The stiffness of the girder is characterized in this report by the load-strain relationships of the elements and by the deflection of the member under load. The primary features which influenced stiffness were (a) the mechanical and geometric properties, (b) the web plates, and (c) the joints at interconnecting elements.

Effects of Mechanical and Geometric Properties

Elastic strains and deflections of a structural member are affected directly by the elastic modulus of the material. As shown in Figure 11 the tensile moduli and material composition varied for the different specimens. Improvement in the axial modulus appeared to be influenced by glass content as evidenced by comparing TTG-2 and TTG-4, and by tension on the strand during winding as evidenced by comparing TTG-4R and TTG-4. The appropriate modulus value was used for each specimen when computing theoretical values for elemental stress or deflection of the panel points. Cross-sectional areas of the wound truss element consisted of strands obtained by multiplying the number of strands in the element by the experimentally determined area of a single strand. The areas of the strands varied somewhat depending upon the resin content and the tension applied to the strand during winding.

Experimental load-strain data are shown in Figure 12 for specimen TTG-3, which are typical for all of the open-web specimens. These data are presented exactly as obtained from the strain indicator to demonstrate the near linearity exhibited and the differences in the strain magnitudes of the different truss elements of the member. The zero shift shown on the load axis was due to a slight preload and friction characteristics of the hydraulic jacks used for loading. Efforts were made to achieve equal strains in all tensile elements in the design of specimens TTG-4,-4R and 5 by adjusting the cross-sectional areas to the stresses predicted by the computer analysis. Some improvement was made for a few elements, but the fabrication procedures and the inexact correspondence of the mathmatical model with the experimental load test prevented much overall improvement in this regard. Figure 13 compares some of the experimental strain data with those obtained from the theoretical study. These data are representative of all the results from all the the specimens and indicate that the theoretically predicted values ranged from 75 to 85 percent of the experimental measurements. These deviations are believed to result primarily from slight movements in the joints which were unaccounted for in the analytical model.

A comparison of the theoretical and experimental load-deflection relationships is shown for three panel points for TTG-4R in Figure 14. Again it is noted that the experimental data indicate larger deflections than those predicted by the theoretical analysis. If, as suggested for the elemental strains, the lack of agreement was due to joint movement, the movement was both elastic and proportional to the load intensity. The measured deflections consistently returned to a zero value upon removal of the load and increased linearly with increasing load. Figure 15 presents comparative load-deflection data for the center point of TTG-5 and also indicates the close agreement of the measured centerline deflections in specimens TTG-3,-4,-4F and -5. It will be recalled that the truss configurations of these specimens were nearly identical (TTG-4, -4R and -5 had even panels and TTG-3 had uneven panel lengths) with variations in their top flange assemblies only. It will also be recalled that the ultimate loads
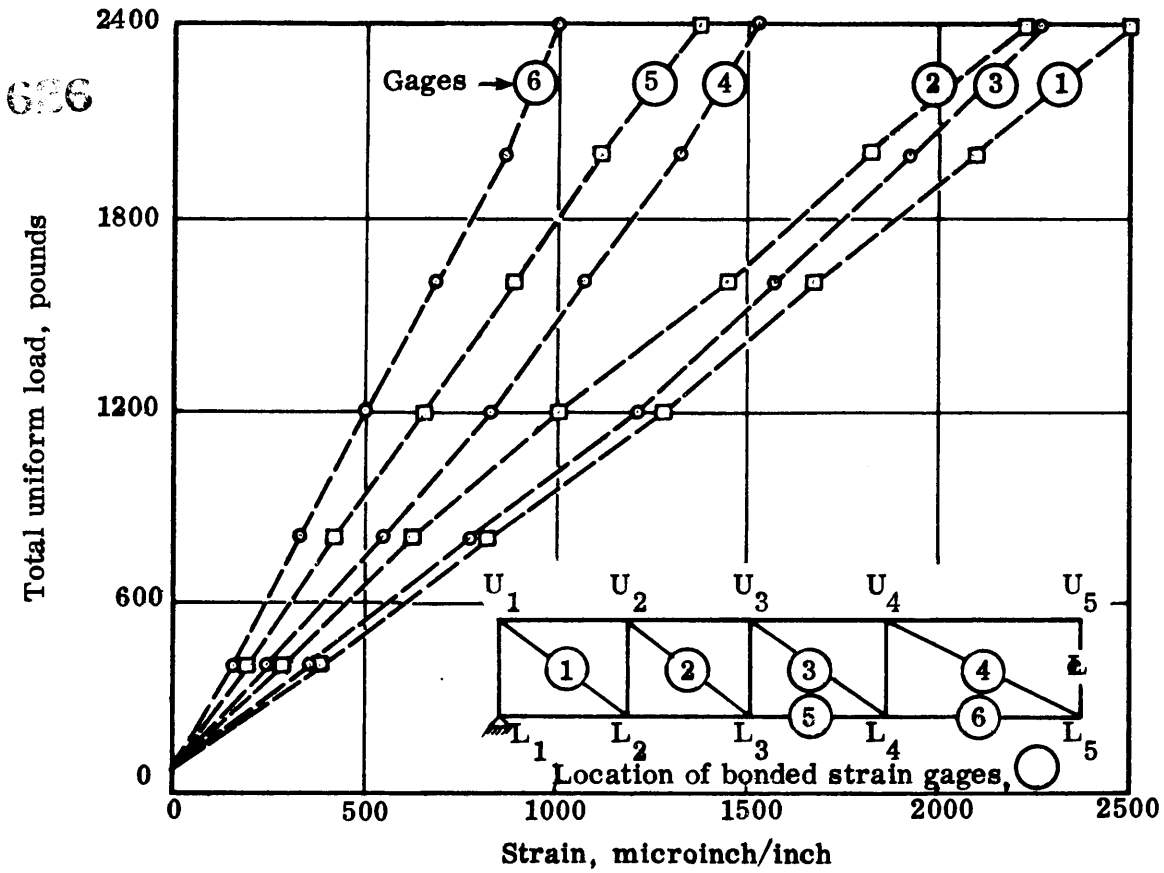
Figure 12.   Load-strain data from instrumented elements in TTG-3.
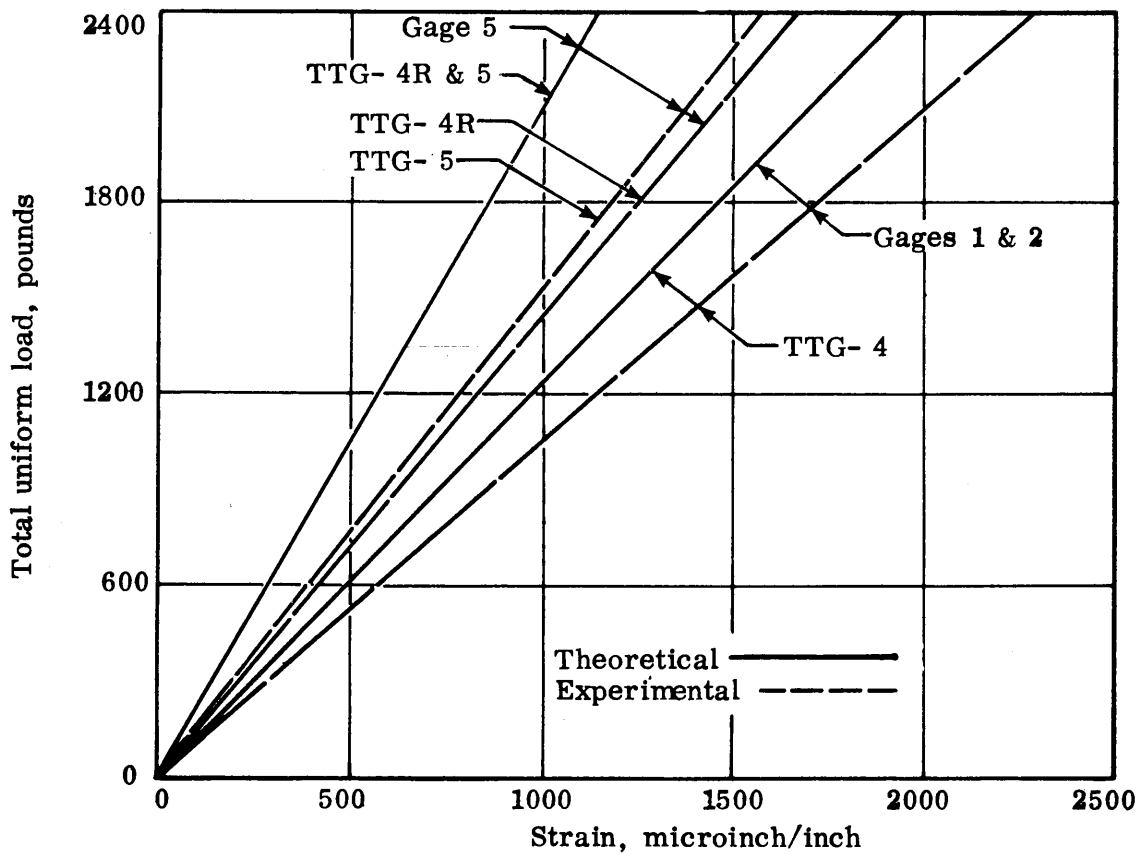

Figure 13.   Load-strain data from instrumented elements in indicated specimens.
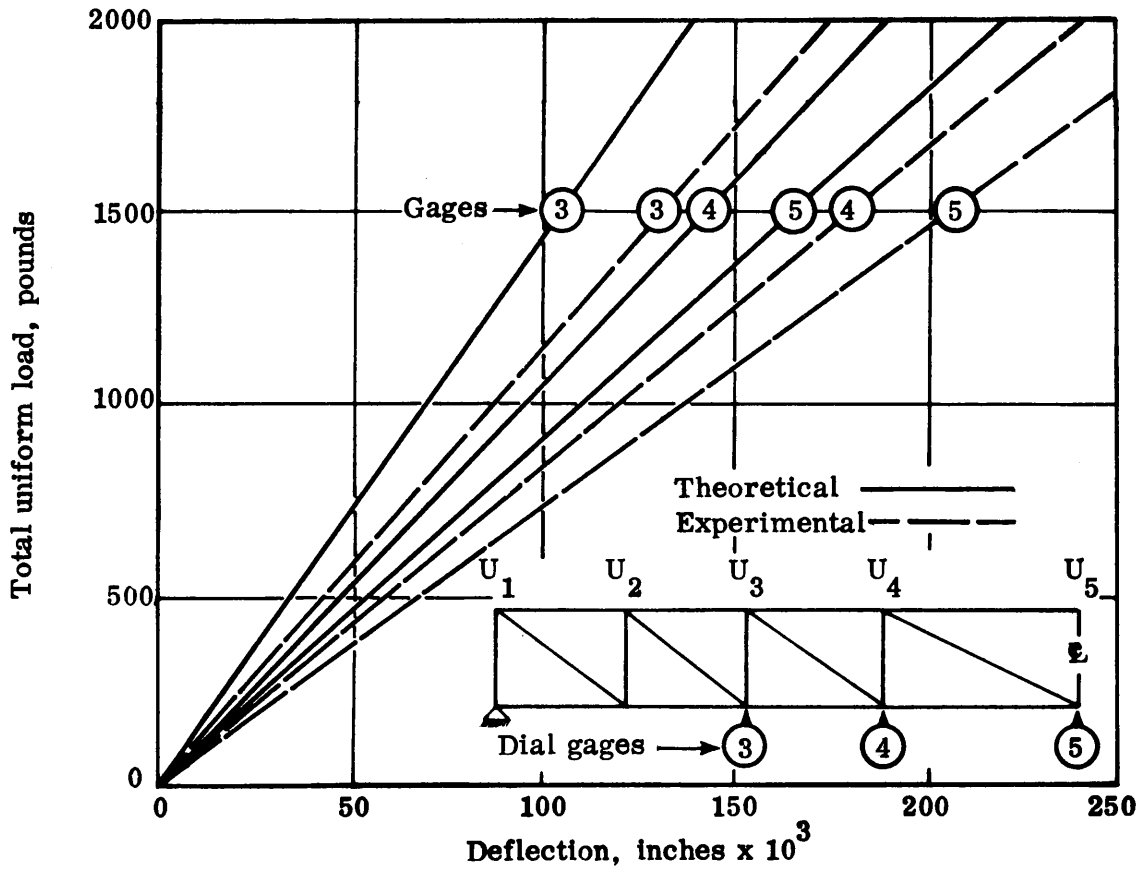
Figure 14.   Load deflections at panel points in TTG-4R.
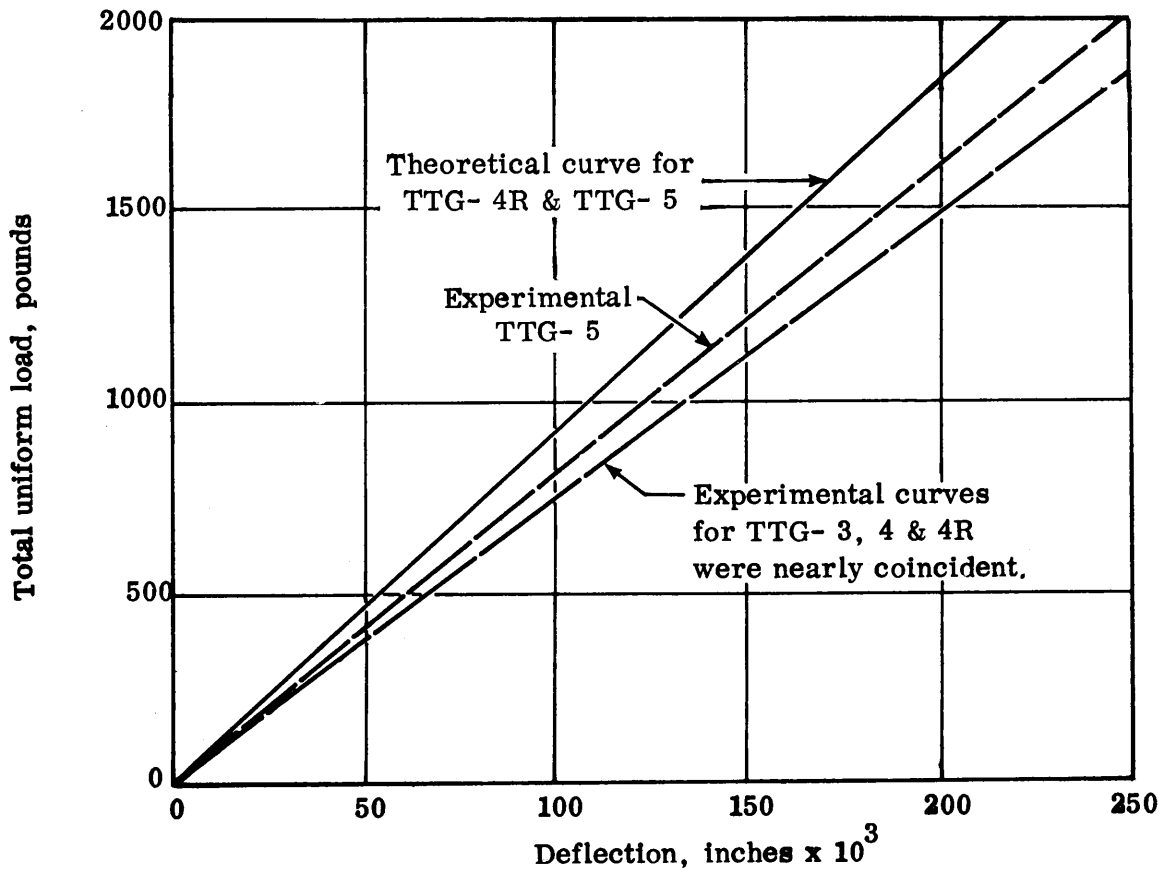

Figure 15.   Load deflections at centerline of indicated specimens.

and the modes of failure of these specimens were quite different. The similarity of the centerline deflection data therefore strongly suggests that the deflection behavior of the girder was governed by the web and lower chord elements only. Improvement in the load-defelection characteristics logically would be achieved by modifying the truss portion of the girder. The data of Figure 15 indicate that a centerline deflection of approximately 0.10 inch (0.25 cm) would be expected at a design load of 100 psf (4.8 KPa). This compares favorably with a value of 0.32 inch (0.80 cm) allowed by structural criteria for comparable terms.

While complete agreement was not achieved between the experimental strain and deflection measurements and those predicted by the theoretical analyses, the agreement was close enough to use the computer analysis to study parameters such as panel size and number, angle of inclination between the web planes, girder span-to-depth ratios, slope of diagonal web members, and areas required for equivalent stress development in the tensile elements. It was on the basis of these computer studies that the several modifications described previously were made.

Effect of Web Plates

The initial design concept for the flexural member was a hybrid combination of both stranded web elements and thin solid web plates. The primary function of the plates was to provide an in-place form to hold the vertical stiffeners in position and to act as a "mandrel" for winding the web and lower chord elements. Subsequent to the fabrication and test experiences with TTG-1 and TTG-2, it was decided that the web plates were not required for fabrication purposes, they did not contribute to the ultimate strength of the member, and they did increase the cost and weight (by 31 percent) of the member. The plates were therefore removed from specimens following TTG-2 and emphasis was place upon studying the behavior of the open web member as a more efficient structural unit. Significantly, however, it was determined that the web plates exerted a strong influence on the deflections of the members with reduction of about 65 percent when compared with TTG-3 at low loads. This effect would undoubtedly disappear, or certainly be reduced substantially, at higher loads or for different plate sizes. A complete description and analysis of the contribution of the web plates when used in conjunction with the trussed webs were reported in the reference cited on Page 1. Verification of these findings was achieved by constructing and testing a girder of the same dimensions as the TTG specimens but in which only the top plate assembly and two solid web plates were used. The experimental deflections of the plate girder were reasonably close to those which were predicted from the computer analysis.

Effect of Joints

The ultimate strength of all test specimens, with the exception of TTG-5, was limited to the strength of the joints. In each of the joint failures, the weak link was the strength of the polyester resin used to bond mating surfaces together. An epoxy adhesive with better bond strength was not used purposely to avoid the introduction of another material and processing variable into the fabrication procedure. The use of a mechanical connection (e.g., the glass strands attaching the channels and plates in TTG-5) was considered to be a more desirable alternative because it involved the same materials and the assembly procedure could be mechanically performed. A quantitative resistance of the joints to internal deformation or external movement, particularly at high loads, was not determined from observation or

or measurement. Therefore, the effect of the joints upon the stiffness of the member can be deduced only qualitatively from the strain and deflection data and inspection of the joints after loading. Figures 13 through 15 compare theoretical and experimental values which indicate that in every case the experimental values exceeded the predicted values at a given load. The theoretical model assumed no internal joint deformation nor displacement which is not allowed in a classical pinned-end truss analysis. Actual movement in or by the joints would therefore result in greater cumulative deflections and stress redistribution in the elements than would be predicted by the theoretical analysis. Considerable "popping" and "cracking" sounds could be heard during the load tests of the specimens, in some cases at loads of about one-half the ultimate. Undoubtedly, some of these sounds orginated in the joints as bonded surfaces ruptured under high strains. Post-failure inspection of joints frequently revealed areas of delaminated fibers or other indications of localized ruptured surfaces but it was usually difficult to determine if the damaged regions were initial or secondary points of failure.

OTHER STRUCTURAL CONSIDERATIONS

Optimum Weight - Strength Characteristics

The research objective of maximizing the live-to-dead-load ratio was not satisfied completely. Only about one-third of the strength potential of the oriented glass strands was developed in the web and chord elements. Further improvement in the strength of the joints and additional adjustment in the cross-sectional areas of the elements to equalize working stresses will increase the live load capacity with little increase in the overall weight of the member. The highest ultimate live- to dead-load ratio was 93 to 1, which was achieved in TTG-5.

Manufacturing Feasibility

Throughout the development and fabrication of the test members consideration was given to the feasibility of manufacturing similar members by automated machines with mass production techniques. The development of the member did not reach a state where it was considered worthwhile to obtain detailed estimates from manufactureres relative to tooling cost, production schedules and other factors. However, contacts were pursued with principals in the following manufacturing and fabricating firm:

1. Morrison Molded Fiber Glass Company
   Bristol, Virginia

2. Plywood and Plastics Corporation
   Richmond, Virginia

3. The Eshbaugh Corporation
   Willow Gove, Pennsylvania

4. Owens Corning Fiberglas Corporation
   Granville, Ohio

These conferences resulted in preliminary assurances, without any estimates of cost involved, that the geometrics and assembly sequences of the flexural member would not present insurmountable manufacturing difficulties. Willingness was expressed to offer assistance as may be required in obtaining cost estimates, technical information, and material sources. Based upon these communications, it appears that the currently conceived configuration of the TTG member would lend itself to industrialized manufacturing procedures.

WEATHERING CONSIDERATIONS

Introduction

Reinforced plastics, along with all other construction materials, are susceptible to the ravages of time and the destructive elements of nature. Approximately one-fourth of all plastics manufactured for public consumption are used in products which are exposed to weathering conditions.[11] A significant body of knowledge has been developed over the past two decades which includes observations of natural and artificial weathering effects, theoretical studies and experimental investigations. A considerable portion of the weathering information found in the literature pertains to thermoplastic materials. However, many of the same principles involved in the process of degradation also apply to thermosetting resins and the data are therefore useful in an evaluation of conventional reinforced plastic composites. Typical documents from the technical literature are referred to in the following discussion.

Pertinent to a study of the outdoor durability of glass-reinforced resin systems is the recognition of the agents which influence the deterioration of the material. Primarily, the ones which contribute to weathering action and which will be considered here in some detail are (a) light, (b) temperature, (c) moisture, and (d) atmospheric gases. All of these agents affect both the glass reinforcement and the resin components of the composite either directly or indirectly, but each agent may affect each component in a different way under the same or differing mechanical or physical conditions. In addition, a combination or an interaction among the major weathering agents within the composite structure frequently produces complex results which may accelerate deteriorative processes. The physiochemical interaction of the weathering factors and the material components account for the difficulty of duplicating natural weathering in a simulated environment. It is therefore not surprising that poor correlations exist between laboratory and field studies of weathering effects. [13, 14, 15] Current industry efforts are directed toward combating weathering effects by providing light absorbing additives to the resin component, by formulating resins which are less permeable to water, and by providing finishes on the glass fibers which protect the reinforcement from chemical attack and assure strong bonds at the resin-glass interface to resist stresses induced by cyclic thermal effects.[16]

A recent study characterized the breakdown of a glass fiber reinforced resin composite as occurring in four distinct chronological steps as follows: [17]

1. Fibers near the surface of the material cause ridges to form in the resin along their length. This is referred to as "fiber ridging". It is believed that swelling of the matrix due to absorption and the chemical action of water cause debonding and displacement of the fiber toward the surface. Dimensional changes due to temperature variations may also be a contributing factor to fiber ridging.

2. The thin layer of resin covering the surface fibers ruptures and thereby exposes the glass fiber directly to the atmospheric environment. Stress fatigue is thought to be a prime cause of resin rupture. However, adverse effects of hydrolytic scission of the polymers and cleavage of bonds due to ultraviolet light may occur simultaneously and accelerate the failure process.

3. Localized spalling and erosion of the resin at the points of rupture follow the formation of cracks. Mechanical actions due to factors such as freezing of water, the impact of rain, wind, and temperature changes hasten the wearing away of the protective resin surface. As erosion continues, bare fibers of glass may be seen protruding from the surface of the underlying matrix resin. This condition is referred to as "fiber prominence".

4. A network of microcracks form in the resin which divides the surface into small, four-sided areas. The regular form of these microcracks differentiates them from a "craze" type of crack pattern and apparently form to relieve multiaxial tensile stresses in the surface material. The "V" shape of the cracks indicates that either the surface stresses diminish toward the bulk material or the strength properties of the resin itself differ considerably through a thin surface layer. Quite likely, the chemical and photolytic processes have altered the structure of the polymer at the surface over the period of exposure so that it becomes increasingly brittle and more susceptible to failure by cyclic stresses. Interestingly, the "V" cracking does not occur until after fiber prominence has become extensive.

Light

Effects on Resin

Photodegradation occurs in organic resins due to the absorption of ultra-violet light in the wave length region of 2800 A^o to 4000 A^o. Carbonyl groups (. COOH) making up the polymer chains are particularly susceptible to degradation since they absorb radiation of 2800 A^o and since the carbon to carbon single bond energy of 80 K cal/mole corresponds to the 100-70 K cal/mole energies of ultraviolet radiation. [18] Structural damage occurs in the polymer primarily due to chain scission and crosslinking. Chain scission results in

a molecular weight reduction due to breaking of the main chain bonds. Crosslinking results in a redistribution of the molecular weights of the polymers from that in the original structure and may cause embrittlement through the development of an infinite structure. Correlation studies have shown that the mechanical properties of tensile strength and ductility are reduced with reductions in molecular weight and crosslinking. [19]

The primary source of natural ultraviolet radiation is direct sunlight. However, reflected sunlight may also contain sufficient intensities of ultraviolet radiation to degrade the resin. Extensive studies have shown considerable variation in the intensity of incident degrading radiation throughout the United States. [19] Those sections of the country with clear atmospheres for much of the year present severe photodegradation problems for reinforced plastics. Notable among these are the midwestern states, and particularly Arizona. The time-intensity relationship of exposure to ultraviolet radiation is critical to the alteration of the resin and therefore, the rate of degradation varies at a particular geographic location with the seasons and with the surface orientation of the structure to the incident light source.

Effects on Glass

There has been no conclusive evidence presented which indicates significant photo-degradation of the glass fiber reinforcement itself. Therefore, no considerations are made for this factor in design procedures, but it should be remembered that the loss of mechanical strength or the protective shield of the resin adjacent to the glass fibers will result in increased stress development in the fibers. In this regard, ultraviolet radiation may be considered an influential factor in the stress condition of reinforcing fibers.

Effects on Composite

The overall effect of exposure to light upon the composite system is the summation of the effects upon the resin in its role as a structural component and as a protective coating for the glass.

Temperature

Effects on Resin

The upper safe working temperatures for general purpose polyester resins range from 300° F to 350° F (149° to 177° C) and for epoxy resins from 250° F to 550°F (121° to 280° C). [20] Outdoor temperature measurements in the United States have ranged from -60° F to 170° F (-51° to 77° C). Therefore, the maximum elevated exposure temperature would not have sufficient thermal energy to cause direct bond cleavage in commercial polymers. However, slightly elevated temperatures may increase degradative rates due to other mechanisms (e.g., oxidation and hydrolysis) and should be considered in these cases. Mechanical properties may be affected adversely to some degree by usual outdoor temperatures but direct temperature effects are not considered significantly detrimental to the structural properties of the resins. Continuing technological advancements in resin formulations have produced some polyesters with stable thermal properties at 600° F (316° C) [21] In

- 24 -

general, reduced temperatures tend to enhance the mechanical properties of resins and also materially reduce the effects of other degrading factors such as water when the temperatures drop below freezing. A rule of thumb applied to polymeric materials stipulates that the thermal life expectancy is doubled when the temperatures is decreased by 15° F to 18° F $(-9^{\circ}$ to -8° C).

Effects on Glass

The elevated temperatures required to change the properties of glass fibers are in excess of $1,000^{\circ}$ F (538° C). Therefore, no direct adverse effects are anticipated due to heat in the glass components of the composite system. Low temperature extremes are equally as ineffective.

Effects on Composite

A detrimental interaction between the resin matrix and the glass fibers may result from temperature changes. The coefficients of thermal expansion and contraction for the two materials may differ by as much as 20 times. Therefore, very large stresses may be generated at the glass-resin interface due to temperatures different from those at which the composite was cured. If the bond strength of the coupling agents at the interface is insufficient to resist the thermal stresses, failures will occur and microcracks will form to create discontinuities in a composite structure.

Moisture

Effects on Resin

Water degrades the strength and integrity of the resin matrix by at least three mechanisms. These include (a) chemical processes such as embrittlement by hydrolysis and leaching of resin additives, (b) physical processes such as internal shrinking and swelling and erosion of surface, and (c) photochemical processes such as the generation of hydroxyl radicals. [22] The role of the resin as a protective shield for the reinforcement may be thwarted to various degrees by the permeation of water molecules through the matrix material to sites on the glass surface. Experimental studies have indicated that different polyester species differ widely in their water permeation rates. Transmission mechanisms are by both diffusion through the matrix and by flow along the fiber-resin interface (referred to as "wicking") in the composite structure. [23] Cyclic absorption and desorption of moisture by the resin may cause dimensional changes which result in progressive bond failures at the resin-glass interface. Similar mechanical damage may result from the freezing and thawing of water which has accumulated in voids or microcracks within the matrix. Studies of moisture absorbed by resins during the storage of raw materials under high humidity conditions have indicated subsequent adverse effects upon the mechanical, electrical, and geometric properties of the finished products. It was concluded in these studies that moisture-inhibited' curing of the resin accounted for some of the property changes. [24]

634

Effects on Glass

The degrading effect of water on unprotected glass fibers has been well documented with observations of tensile strength reductions of up to 50 percent over short periods of time. Degradation of the glass is a complex process involving factors such as the composition of the glass itself, the character of the "size" applied to the fiber, the stress in the fiber, temperature, moisture adsorbed by the glass, and the dimensions of the fiber. [25] For example, the geometric effect of the fiber is shown by comparing the weight loss of a fiber to that of bulk glass due to the chemical action of water. The weight loss of a 0.4-mil (10u) diameter fiber proceeds at a rate of about 700 times that of bulk glass due to the relatively larger surface area of the fiber. [26]

Effects on Composite

The connecting link between the resin matrix and the glass reinforcement is the coupling agent (sometimes referred to as "size" or "finish") applied to the glass fiber as it emerges from the bushing during manufacture. Coupling agents are selected for compatibility with the resin matrix and are usually chemical formulations containing a modified chrome complex or a vinyl silane compound. The effectiveness of the coupling agents in preventing moisture attack on the glass fibers with a concomitant destruction of the interfacial bond and reduction in mechanical properties has been clearly demonstrated. [27] Since most structural composites contain less than 50 percent resin by weight, glass fibers near the surface of the material normally have a thin resin cover. Therefore, common practice is to provide a relatively thick (10 to 30 mil) (.25 to .75mm) coating of resin referred to as a "gel coat" for protection to the exterior surface of the composite for protection of the underlying material from moisture, light, erosion, temperature and abrasion. Gel coats may be composed of the same resin as that used for the matrix or of a different resin. Seal coats such as polyurethane containing colorants and ultraviolet absorbers have been used recently for additional protection for exposed surfaces. [28,29] Therefore, three lines of defense may be provided for the protection of the reinforcement: the resin matrix, the surface coating, and the coupling agent on the fiber.

Oxidation and Atmospheric Gases

Effects on Resin

Rapid degradation processes which are associated with atmospheric gases such as ozone are usually coupled with ultraviolet light effects. Thus, "oxidizing" (used generically here to apply to several gaseous reactions) processes are frequently characterized as photo-oxidation reactions. Thermal-oxidation reactions may also occur in the absence of light, with the rate of degradation dependent upon the temperature level. Crosslinking of polymers, accompanied by increased embrittlement is more pronounced in the photo oxidation than in the thermal-oxidation reactions. The penetration of gaseous molecules into the resin and subsequent reaction with free radicals or chain segments result in losses in optical, dielectric, and mechanical strength properties. [30] The rate of oxidation is controlled by the rate of

diffusion of a gas into the bulk polymer, assuming that light radiation and temperature are constant. Diffusivity is a function of the crystalline structure of the polymer, so the oxidation process is self-retarding as the crosslinking and increased crystallinity occur.

Effects on Glass

A direct reaction between the surface of the glass reinforcement and gas molecules does not constitue a problem in structural plastics. Chemical reactions resulting from atmospheric gases dissolved in moisture contained in the resin matrix may possibly result in reduced strengths but no substantial evidence of this source of degradation appears in the literature.

Effects on Composite

The reduction in performance of the composite material is related to the detrimental effects of atmospheric gases upon the resin matrix.

Summary of Weathering Effects

When the various factors which make up the effect of outdoor exposure are considered as a whole, the following generalizations may be stated based upon the current state of knowledge in the area of weathering. [27]

1. Decreases in strength properties (tensile, compressive, and flexural) for the general purpose resin range from 20 to 30 percent over periods of 3 to 10 years.

2. Heat and fire resistant resins may lose up to 10 percent more strength than the general purpose types in the same time period.

3. Materials containing styrene cross-linkers will inevitably suffer changes in optical properties with aging and exposure.

4. Most current evidence indicates that weathering effects are not accelerated by mechanically prestressing the composite up to 40 percent of its ultimate strength before exposure. Weathering while under stress may or may not be accelerated. Data appear to be contradictory on this point.

5. Biological attack may be ignored as a degrading element of the environment.

6. Materials improvements such as using crosslinkers other than a styrene are being explored and implemented. The evaluation of improvements necessarily must await the test of time in outdoor exposure conditions to determine accurate results.

An accurate estimate of the useful life of structural plastic is still unpredictable. The first polyester resin was synthesized 30 years ago and the first epoxy resin was accepted as a structural resin only 20 years ago. Therefore, long-term test data on recently improved composite materials are nonexistent and opinions of service life vary. Some estimates predict 10 to 15 years of life in severe exposures and 30 years in temperate climates. Anticipating further technological improvements, other predictions forecast a life of 60 years as commonplace. [9,31] In addition to improvements in the materials themselves and in acceletated test methods, considerable progress has been made with simulated computer models which provide theoretical weathering data for complex systems in short periods of time. [32]

CONCLUSIONS

The limited scope of the laboratory studies provided few comprehensive conclusions relative to the overall consideration of the use of high performance plastics in highway structures. However, data were obtained which demonstrated or suggested the following conditions or relationships.

1. Classical design and analytical procedures based on a pinned-end truss configuration were in reasonably close agreement with the experimental strains and deflections measured during load testing of the open-web members.

2. Measured strains and deflections in the members varied linearly with load over the test range.

3. The elastic tensile modulus of the stranded material increased with increased glass content and presumably with increased strand tension during fabrication.

4. Initial failure of all specimens occured in the top plate assembly and thereby precluded the determination of the ultimate strength values of the elements or the behavior of the member at high loads. A maximum value of 93 to 1 was achieved for an ultimate live-to dead-load ratio.

5. Predictable life spans for structural plastics exposed to natural weathering conditions are uncertain as of this time. Efforts are continuing by industrial interests to improve materials properties and performance data are being compiled from numerous sources. It is anticipated that design recommendations and predictions for service life spans will be enhanced with the passage of time.

REFERENCES

1. Brown, H.C., "Plastics in Construction," Civil Engineering, Vol. 39, No. 8, August 1969, pp. 39-41.

2. Davies, R.M., Plastics in Building Construction, Blackie & Son, Ltd., London and Glasgow, 1965.

3. Dietz, A.G.H., Plastics for Architects and Builders, The MIT Press, Cambridge, Massachusetts, 1969.

4. Skeist, Irving, ed., Plastics in Building, Reinhold Publishing Corporation, New York, 1966.

5. "All-Plastics Pedestrian Bridge Built in England", Modern Plastics, Vol. 47, No. 3, March 1970, p. 164.

6. McCormick, Fred C., "Why Not Plastic Bridges?", Journal of the Structural Division, ASCE, Vol. 98, No. ST8, August 1972, pp. 1757-1767.

7. Baer, Eric, ed., Engineering Design for Plastics, Reinhold Publishing Corporation, New York, 1964.

8. Benjamin, B.S., Structural Design with Plastics, Van Norstrand Reinhold Company, New York, 1969.

9. Parkyn, Brian, ed., Glass Reinforced Plastics, CRC Press, The Chemical Rubber Company, Cleveland, Ohio, 1970.

10. Rosato, D.V., and C.S. Grove, Jr., Filament Winding, Interscience Publishers, Division of John Wiley & Sons, Inc., New York, 1964.

11. Rosato, D.V., "The Weatherability Market - 25% of All Plastics Growing," Plastic World, Vol. 25, No. 7, July 1967, pp. 36-47.

12. "Weathering Effects on Plastics", Tech News Bulletin, U.S. National Bureau of Standards, Vol. 53, No. 8, August 1969, p. 171.

13. Grensfelder, Henry, "Analysis of Plastic Weathering Results," Symposium on the Weatherability of Plastics, Gaithersburg, Maryland, Interscience Publishers, New York, 1967, pp. 245-262.

14. Samson, G.G., "Evaluation of Environmental Performance of Plastics Materials and Mouldings", Applied Polymer Symposium, No. 17, John Wiley & Sons, Inc., 1971, pp. 201-212.

15. Kamal, M.R., "Evaluation of the Weatherability of Plastics", SPE Regional Technical Conference, Philadelphia, Pennsylvania, October 1972.

16. Czarnomski, T.J., "Unsaturated Polyester," Modern Plastics Encyclopedia, 1973-74, pp. 66-68.

17. Blaga, A., "Weathering Study of Glass-Fiber Reinforced Polyester Sheets by Scanning Electron Microscopy", Polymer Engineering and Sciences, Vol. 12, No. 1, January 1972, pp. 53-58.

18. Jellinek, H.H.G., "Fundamental Degradation Process Relavent to Outdoor Exposure of Polymers," Symposium on the Weatherability of Plastics, Gaithersburg, Maryland, Interscience Publishers, New York, 1967, pp. 41-59.

19. Hamel, M.R., "Cause and Effect in the Weathering of Plastics," Polymer Engineering and Science, Vol. 10, No. 2, March 1970.

20. Modern Plastics Encyclopedia, McGraw-Hill, Vol. 50, No. 10-A, October 1973, p. 540-550.

21. Cottis, S.G., "High-Temperature Aromatic Polyester," Modern Plastics Encyclopedia, 1973-74, pp. 68-70.

22. Kamal, M.R., and Robert Saxon, "Recent Developments in the Analysis and Prediction of the Weatherability of Plastics," Symposium on the Weatherability of Plastics, Gaithersburg, Maryland, Interscience Publishers, pp. 1-28.

23. Regester, R.F., "Behavior of Fiber-Reinforced Plastic Materials in Chemical Service," Corrosion, Vol. 25, No. 4, April 1969, pp. 157-167.

24. Conway, J.M., "Effects of Moisture in Thermosets on Finished Product Properties," Modern Plastics, Vol. 50, No. 7., July 1973, pp. 65-68.

25. Otto, W.H., "The Effects of Moisture on the Strength of Glass-Fibers—A literature Review," Research Report, Whittaker Corporation, Narmco R & D Division, San Diego, California, June 1965.

26. Broutman, T.J., and R.H. Krock, Modern Composite Materials, Addison-Wesley, 1967, pp. 298-299.

27. Rugger, G.R., and J.B. Titus, "Weathering of Glass Reinforced Plastics", Plastics Technical Evaluation Center (PLASTEC), Picotinny Arsenal, Dover, New Jersey, PLASTEC Report 24, January 1966, p. 169.

28. Green, D.H., and P.R. Guevin, "Polyurethanes—The New FRP Finish", Proceedings of the 28th Annual Technical Conference, The Society of the Plastics Industry, Inc., January 1973, pp. 1-6, Section 8-B.

29. Winfield, A.G., "RP in Construction Rises High Down Under," Modern Plastics, Vol. 49, No. 6, June 1972, pp. 62-63.

30. Winslow, F.H., and W.L. Hawkins, "Some Weathering Characteristics of Plastics," Symposium on the Weatherability of Plastics, Gaithersburg, Maryland, Interscience Publishers, New York, 1967, pp. 29-39.

31. Scott, K.A., "Plastics", The Weathering and Performance of Building Materials, Chapter 6, Wiley-Interscience, A Division of John Wiley & Sons, New York, 1970.

32. Rosato, D.V., and R.T. Schwartz (ed.) Environmental Effects on Polymeric Materials, Vol. 1, Chapter 9, John Wiley & Sons, New York, 1970.

APPENDIX A

STRESS ANALYSIS AND DESCRIPTION OF COMPUTER PROGRAM

Axial stresses in the web and lower chord elements and displacements at the joints were computed theoretically by a strain-energy method utilizing stiffness matrices which were adapted for solution by a digital computer. The force-displacement relationship was

$$q_i = \sum_{j=1}^{n} k_{ij} d_j$$

where $i = 1, 2, ---, 4$; q is a force vector on a truss element with 4° of freedom; the stiffness coefficient, k_{ij}, is the force that must be applied in a direction i to produce a unit deformation in direction j when all other deformations of the elements do not change; d is the deformation of each element in the system. Expressed in matrix notion, the relation becomes

$$\{q\} = [K]\{d\}$$

It is convenient to indicate that the deformations of the elements with reference to their own geometric axes, u and v as shown in Figure A-1. The stiffness matrix of a single element of the truss then becomes

$$[K] = \frac{AE}{L} \begin{bmatrix} 10 & -10 \\ 00 & 00 \\ -10 & 10 \\ 00 & 00 \end{bmatrix}$$

The stiffness matrix $[K]$ of the entire truss may be generated by superposition of the matrices of each element. However, in order to apply the principle of superposition, it is necessary to transform the stiffness matrices of the elements to a global set of axes, x and y, as shown in Figures A-1. The transformation may be accomplished by the matrix T:

$$[T] = \begin{bmatrix} m & +n & o & o \\ -n & m & o & o \\ o & o & m & n \\ o & o & -n & m \end{bmatrix}$$

where $m = \cos \alpha$ and $n = \sin \alpha$ with α as shown in Figure A-1.

Thus $\{q\} = [T]\{q\}_{xy}$

and $\{d\} = [T]\{d\}_{xy}$

Figure A-1. Directional axes for each truss element.
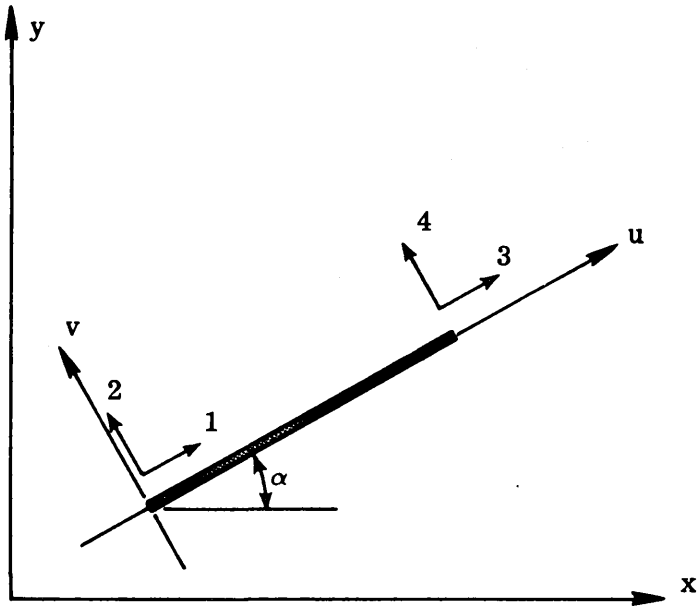
Legend
x, y global axes
u, v element axes

Numbers indicate displace-
ments of ends of elements
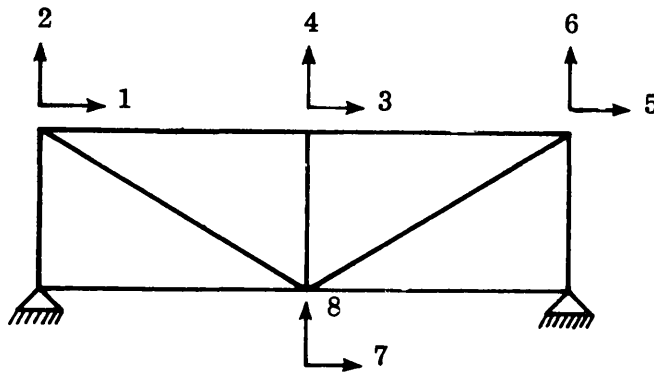
Note: Numbers indicate displacements of joints

Figure A-2. Typical displacement directions of joints
in the truss. The numbers refer to
independent possible motions.

A-2

Substitution of the transformed u v matrices and solution for the xy stiffness coefficient gives

$$\left[K\right]_{xy} = \left[T\right]^T \left[K\right] \left[T\right]$$

If the external forces and corresponding displacements of the joints in the truss are denoted by $\{Q\}$ and $\{D\}$ respectively, the matrix equation for the load-displacement relationship of the entire truss may be shown as

$$\{Q\} = \left[K\right] \{D\}$$

Figure A-2 shows schematically the set of directions by which the forces and displacements were defined. For a given load vector $\{Q\}$, this set of linear simultaneous equations may be solved for $\{D\}$. Thereafter, the deformation vector (d_{xy}) of each element can be obtained. Subsequent multiplication of $\{d_{xy}\}$ by $\{K\}_{xy}$ gives values for $\{q\}_{xy}$ as desired. The final axial and transverse stress in each element is obtained by transforming the xy components into the directions by

$$\{q\} = \left[T\right] \{q\}_{xy}$$

Final values are presented in unit stresses and strains.

Final computations are printed as axial stress and strain for each element and the deflections of each panel point. A complete statement of the computer program is included in the following pages.

```
                 PROGRAM FRAME(INPUT, OUTPUT, TAPE5=INPUT,TAPE6=OUTPUT,TAPE1)
000003           DIMENSION TITLE(20),S(30,30),P(30),NCODE(20,6),SM(6,6),DM(6),D(30)
000003           DIMENSION           PM(6),PMI(6),T(6,6)
000003           DIMENSION SIG(20),EPS(20)
000003       999 READ(5,1)(TITLE(J),J=1,20)
000015         1 FORMAT(20A4)
000015           WRITE(6,2)(TITLE(J),J=1,20)
000027         2 FORMAT(IH1,///20X,20A4)
000027           READ(5,5)ME,N
000037         5 FORMAT(2I5)
000037           READ(5,10) E  ,APS
000047           WRITE(6,7) E  ,APS
000057         7 FORMAT(///25X,19HMOD. OF ELASTICITY=,F10.1/25X,19HAREA PER STRAND   =
                I  =,F10.6)
000057           READ(5,10)(P(J),J=1,N)
000072        10 FORMAT(8F10.2)
000072        41 FORMAT(6F10.0)
000072           DO 15 I=1,N
000074           DO 15 J=1,N
000075        15 S(I,J)=0.
000104           WRITE(6,19)
000107        19 FORMAT(///6X,8HMEMB.NO.,2X,5H AREA,2X,11H MOM. INER.,11H HOR. COMP
                1.,11H VER. COMP.,3X,25H CODE NUMBERS OF EACH BAR)
000107           MTAPE=1
000110           REWIND MTAPE
000112           DO 20 M=1,ME
000114           READ(5,33)A,XI,Y,Z,(NCODE(M,J),J=1,6)
000137        33 FORMAT(4F10.0,6I5)
000137           DL=(Y**2+Z**2)**.5
000145           EM=Y/DL
000147           EN=Z/DL
000150           WRITE(6,34)M,A,XI,Y,Z,(NCODE(M,J),J=1,6)
000176        34 FORMAT(8X,I3,F10.4,F10.4,2F10.2,7X,6I4)
000176           CALL MEMST(A,XI,E,DL,EM,EN,SM)
000205           WRITE(MTAPE)SM,EM,EN,A
000220           DO 35 I=1,6
000222           IF(NCODE(M,I).EQ.0) GO TO 35
000225           K=NCODE(M,I)
000230           DO 45 J=1,6
000232           IF(NCODE(M,J).EQ.0) GO TO 45
000235           L=NCODE(M,J)
000240           S(K,L)=S(K,L)+SM(I,J)
000246        45 CONTINUE
000250        35 CONTINUE
000252        20 CONTINUE
000255           WRITE(6,55)
000260        55 FORMAT(///40X,11HLOAD VECTOR)
000260           DO 60 J=1,N
000262        60 WRITE(6,65)J,P(J)
000274        65 FORMAT(40X,2HP(,I2,2H)=,F10.2)
000274           WRITE(6,68)
000277        68 FORMAT(///40X,18HJOINT DEFORMATIONS)
000277           CALL GAUSS(S,D,P,N)
000302           DO 80 I=1,N
000304        80 WRITE(6,85) I,D(I)
000316        85 FORMAT(40X,2HD(,I2,2H)=,F10.7)
000316           WRITE(6,90)
```

```
000321      90  FORMAT(///40X,17HMEMBER END FORCES)
000321          REWIND MTAPE
000323          DO 120 M=1,ME
000325          READ(MTAPE)SM,EM,EN,A
000340          DO 130 I=1,6
000342          DM(I)=0.
000343          PM(I)=0.
000344          K=NCODE(M,I)
000350          IF(K.EQ.0) GO TO 130
000351          DM(I)=D(K)
000352     130  CONTINUE
000354          DO 140 I=1,6
000356          DO 140 J=1,6
000357     140  PM(I)=PM(I)+SM(I,J)*DM(J)
000371          DO 502 I=1,6
000372     502  PMI(I)=0.
000375          CALL TRANS(EM,EN,T)
000377          DO 445 I=1,6
000401          DO 445 J=1,6
000402     445  PMI(I)=PMI(I)+T(I,J)*PM(J)
000414          WRITE(6,447)M,PMI(4)
000423     447  FORMAT(40X,I3,2X,F10.5)
000423          SIG(M)=PMI(4)/A
000426          EPS(M)=SIG(M)/E
000430     120  CONTINUE
000432          WRITE(6,875)(M,SIG(M),EPS(M),M=1,ME)
000450     875  FORMAT(///15X,8HMEMB.NO.,10X,6HSTRESS,10X,6HSTRAIN/(17X,I3,8X,
                1   12E15.6))
000450          GO TO 999
000451          END
```

```
                 SUBROUTINE MEMST(AA,XI,E,DL,EM,EN,SM)
000012           DIMENSION SM(6,6)
000012           A=4.*E*XI/DL
000014           B=A/2.
000016           C=(A+B)/DL
000020           D=2.*C/DL
000022           S=AA*E/DL
000023             SM(1,1)=D*EN*EN+S*EM*EM
000030             SM(2,1)=(S-D)*EM*EN
000032             SM(2,2)=D*EM*EM+S*EN*EN
000035             SM(3,1)=C*EN
000037             SM(3,2)=-C*EM
000041             SM(3,3)=A
000043             SM(4,1)=-D*EN*EN-S*EM*EM
000047             SM(4,2)=(D-S)*EM*EN
000052             SM(4,3)=-C*EN
000054             SM(4,4)=D*EN*EN+S*EM*EM
000057             SM(5,1)=SM(4,2)
000062             SM(5,2)=-SM(2,2)
000064             SM(5,3)=C*EM
000065             SM(5,4)=SM(2,1)
000067             SM(5,5)=SM(2,2)
000071             SM(6,1)=C*EN
000073             SM(6,2)=-C*EM
000075             SM(6,3)=B
000077             SM(6,4)=-C*EN
000101             SM(6,5)=C*EM
000103             SM(6,6)=A
000104           DO 5 I=1,6
000106           DO 5 J=I,6
000107         5 SM(I,J)=SM(J,I)
000121           RETURN
000121           END
```

```
              SUBROUTINE GAUSS(A,X,BB,N)
000007        DIMENSION A(30,30),W(30,32),B(30),X(30),Q(30),P(30),D(30)
000007        DIMENSION S(30,32),BB(30)
       C  SOLUTION OF AX=B BY GAUSSIAN ELIMINATION
000007        DET=1.
000010        NP1=N+1
000012        NP2=N+2
000014        NM1=N-1
       C  FORM VECTORS D AND P
000015        DO 2 I=1,N
000016        P(I)=I
000020        D(I)=ABS(A(I,1))
000022        DO 2 J=2,N
000024        IF(D(I).LT.ABS(A(I,J)))    D(I)=ABS(A(I,J))
000037      2 CONTINUE
       C  ESTABLISH WORKING MATRIX W
000044        DO 3 I=1,N
000045        DO 3 J=1,N
000046      3 W(I,J)=A(I,J)
000057        DO 4 I=1,N
000060        W(I,NP1)=D(I)
000064      4 W(I,NP2)=P(I)
       C  TAKE A COLUMN TO START ELIMINATION
000071        DO 5 J=1,NM1
       CALCULATE AND COMPARE Q*S
000072        QMAX=0.
000073        DO10 I=J,N
000074        Q(I)=ABS(W(I,J))/W(I,NP1)
000103        IF(Q(I)-QMAX) 10,10,8
000106      8 QMAX=Q(I)
000110        M=I
000111     10 CONTINUE
       C  EXCHANGE ROWS IF NECESSARY
000114        IF(M.EQ.J) GO TO 20
000116        DET=-DET
000117        DO 15 JJ=1,NP2
000120        S(J,JJ)=W(J,JJ)
000125        W(J,JJ)=W(M,JJ)
000130     15 W(M,JJ)=S(J,JJ)
       C  TAKE A ROW, CALCULATE M(I,J), STORE IN W(I,J)
000135     20 JP1=J+1
000137        DET=DET*W(J,J)
000142        DO 5 I=JP1,N
000144        W(I,J)=W(I,J)/W(J,J)
       C  ELIMINATION
000151        DO 5 K=JP1,N
000153        W(I,K)=W(I,K)-W(I,J)*W(J,K)
000164      5 CONTINUE
000173        DET=DET*W(N,N)
000176        IF(ABS(DET).LT.1.E-10)    GO TO 705
000201        DO 25 I=1,N
000203        INP2=W(I,NP2)
000207     25 B(I)=BB(INP2)
       C  MODIFY B VECTOR
000213        DO 30 J=1,NM1
000215        JP1=J+1
000217        DO 30 I=JP1,N
```

A-7

```
000221        30 B(I)=B(I)-W(I,J)*B(J)
        C  BACK SUBSTITUTION
000233           X(N)=B(N)/W(N,N)
000240           DO 101 K=2,N
000241           J=N-K+1
000243           SUM=0.
000244           JJ=J+1
000246           DO 115 I=JJ,N
000247       115 SUM=SUM+W(J,I)*X(I)
000256       101 X(J)=(B(J)-SUM)/W(J,J)
000266           RETURN
000266       705 WRITE(6,750)
000272       750 FORMAT(//20X,20HMATRIX A IS SINGULAR)
000272           RETURN
000273           END
```

```
                    SUBROUTINE TRANS(EM,EN,T)
000006              DIMENSION T(6,6)
000006              DO 5 I=1,6
000007              DO 5 J=1,6
000010            5 T(I,J)=0.
000017              T(1,1)=EM
000020              T(1,2)=EN
000021              T(2,1)=-EN
000022              T(2,2)=EM
000023              T(3,3)=1.
000025              T(4,4)=EM
000026              T(4,5)=EN
000027              T(5,4)=-EN
000030              T(5,5)=EM
000031              T(6,6)=1.
000032              RETURN
000032              END
```